Macromolecules
ARTICLE

Macromolecules **2009**, *42*, 7897–7902 **7897**
DOI: 10.1021/ma901313a

Phase Behavior of Polystyrene-*b*-poly(methyl methacrylate) Diblock Copolymer

Hyungju Ahn,[†] Du Yeol Ryu,*[,†] Youngmin Kim,[‡] Kyung Wook Kwon,[§] Jumi Lee,[§] and Junhan Cho*[,§]

[†]*Department of Chemical and Biomolecular Engineering, Yonsei University, 134 Sinchon-dong, Seodaemun-gu, Seoul 120-749, Korea,* [‡]*Department of Electrical Engineering, Hongik University, 72-1 Sangsoo-dong, Mapo-gu, Seoul 121-791, Korea, and* [§]*Department of Polymer Science and Engineering, and Center for Photofunctional Energy Materials, Dankook University, 126, Jukjeon-dong, Suji-gu, Yongin-si, Gyeonggi-do 448-701, Korea*

Received June 18, 2009; Revised Manuscript Received August 30, 2009

ABSTRACT: The phase behavior of polystyrene-*b*-poly(methyl methacrylate) (PS-*b*-PMMA) copolymers of various molecular weights has been studied by using small-angle X-ray scattering (SAXS) and depolarized light scattering (DLS). The empirical Flory χ, determined from scattering intensity profiles for a fully disordered PS-*b*-PMMA copolymer, was shown to behave differently depending on temperature range. χ was described mostly by enthalpic contribution at higher temperatures, but a dominant entropic contribution appeared in χ at lower temperatures. The order−disorder transition (ODT) temperatures for the series of copolymers with the controlled molecular weights were directly measured through SAXS and DLS. The resultant ODTs were then compared with a compressible random-phase approximation theory to determine cross interactions between block components. It was found that effective χ from theory is also mostly described by enthalpic contribution, which yields a moderate change in ODT upon the increase of copolymer molecular weight. In addition, we discussed the pressure response of the copolymer using χ from theory.

Introduction

Interest in nanoscale materials is enormous in all the scientific areas, including polymer science, because a new nanomaterial can lead to a more advanced and efficient technology in various applications such as microelectronic engineering and bioengineering.[1−13] Block copolymers are obtained from connecting two dissimilar polymers by covalent bonding. These polymers can yield well-defined nanostructured materials through self-assembly behavior. Typical nanostructures include classical body-centered or face-centered cubic, hexagonally packed cylindrical, lamellar structures and more complex nonclassical structures with cubic or noncubic network structures.[14−18] There have been in recent decades extensive experimental investigations into the self-assembly behavior of block copolymers[14−17] and also numerous theoretical developments in both conventional field[15,19−27] and molecular approaches.[28−40]

The essence of nanoscale self-assembly in block copolymers lies in the so-called effective Flory interaction χ, which is the dimensionless excess energy on mixing scaled by thermal energy kT. A diblock copolymer with N segments exhibits self-assembled structure or order if $N\chi$ becomes larger than a certain value at each composition.[15,18] The most common method in determining χ is to use phenomenological incompressible theory by Leibler[19] or by Fredrickson and Helfand[21] to fit experimental measurements such as small-angle radiation scattering. Meanwhile, the phase behavior of polystyrene-*b*-poly(methyl methacrylate) (PS-*b*-PMMA) has been widely studied because the copolymer is one of the most useful nanoscopic materials as templates and scaffolds.[7,8,41] The Flory χ of the PS-*b*-PMMA system was first obtained by Russell et al. using small-angle neutron scattering (SANS),[42] and recently it was redetermined in a more thorough SANS study by Ryu et al.[43] or small-angle X-ray scattering (SAXS) measurements for the copolymer by Hashimoto and co-workers.[44] Unlike typical diblock copolymers, it was revealed that χ possesses a strong entropic contribution and relatively small enthalpic contribution. After Russell et al.'s work, the large entropic contribution to χ of the PS-*b*-PMMA copolymer has been attributed by Freed et al. to the entropic effects associated with packing hindrance in the mixture of the two polymers with different pendant group structures.[45,46] When the molecular Lattice Cluster theory was used, it was further shown that the nanoscale self-assembly in the PS-*b*-PMMA system can be suppressed by pressurization (baroplasticity).[45,46] However, the recent investigation on the copolymer by Mayes and co-workers revealed that the applied pressure strengthens the ordering (barotropicity) in molten PS-*b*-PMMA on the contrary.[47]

In this study, we report ordering transition behavior for the PS-*b*-PMMA copolymers of various molecular weights with a fixed composition using SAXS and depolarized light scattering (DLS). The SAXS intensity profiles for a fully disordered PS-*b*-PMMA copolymer are used to obtain empirical Flory χ as a function of inverse temperature. The intensity profiles at temperatures far above glass transition reveals χ mostly described by enthalpic contribution, which is a significant contrast to χ in the literature with the entropic dominance. As temperature is lowered, the newly determined χ begins to have stronger entropic contribution similar to those reported previously. We directly measure ODTs for the copolymers of higher molecular weights through SAXS and DLS. Those measured transition temperatures are analyzed with a compressible random-phase approximation (RPA) theory recently developed by Cho.[36−40] It is found from theory that χ based on ODT is also mostly described by its enthalpic contribution. In addition, it is predicted using χ from

*To whom correspondence should be addressed. E-mail: jhcho@dankook.ac.kr (J.C.); dyryu@yonsei.ac.kr (D.Y.R.).

Published on Web 09/21/2009

Table 1. Molecular Characteristics of PS-*b*-PMMA Diblock Copolymers

sample code	M_n	M_w/M_n[a]	Φ_{PS}	remark (wt ratio)[c]
PS-*b*-PMMA-20.0p	20000	1.05	0.553[b]	pristine (20k)
PS-*b*-PMMA-26.0	26000	1.06	0.546	20k (0.295)/29k (0.705)
PS-*b*-PMMA-26.3	26300	1.06	0.547	20k (0.259)/29k (0.741)
PS-*b*-PMMA-26.8	26800	1.06	0.548	20k (0.196)/29k (0.804)
PS-*b*-PMMA-27.7	27700	1.06	0.550	20k (0.093)/29k (0.907)
PS-*b*-PMMA-28.5p	28500	1.05	0.553[b]	pristine (29k)
PS-*b*-PMMA-29.2	29200	1.07	0.551	36k (0.101)/29k (0.899)
PS-*b*-PMMA-29.9	29900	1.08	0.549	36k (0.192)/29k (0.808)
PS-*b*-PMMA-30.2	30200	1.09	0.548	36k (0.250)/29k (0.750)
PS-*b*-PMMA-30.6	30600	1.09	0.547	36k (0.301)/29k (0.699)
PS-*b*-PMMA-35.6p	35600	1.07	0.536[b]	pristine (36k)

[a] Weight- and number-average molecular weights (M_w and M_n) and polydispersity (M_w/M_n) were measured by size-exclusion chromatography (SEC). [b] Volume fractions of PS for the pristine PS-*b*-PMMA copolymers were measured by ^{1}H nuclear magnetic resonance (NMR). [c] The binary mixtures of PS-*b*-PMMAs were prepared by the freeze-drying method from polymer solution in benzene.

theory that the pressure response of the copolymer is slightly baroplastic initially, then turns to be barotropic, which implies that the increase of unfavorable energetics due to the increased contact density soon prevails as the action of the copolymer against pressure.

Experimental Section

Three PS-*b*-PMMA copolymers used in this study were purchased from Polymer Source Inc., which were synthesized by the sequential anionic polymerization of styrene and methyl methacrylate in tetrahydrofuran (THF) at −78 °C in the presence of LiCl using *sec*-butyllithium as an initiator. The number-average molecular weights (M_n), characterized by size-exclusion chromatography (SEC), were measured to be 20000, 28500, and 35600 g/mol with the polydispersity index (PDI) less than 1.08. PS volume fraction (Φ_{PS}) of the copolymer was determined to be near symmetric by ^{1}H nuclear magnetic resonance (^{1}H NMR) based on the mass densities of two components (1.05 and 1.184 g/cm^3 for PS and PMMA, respectively). The molecular characteristics for PS-*b*-PMMA copolymers and their mixtures used in this study are summarized in Table 1.

To precisely control the molecular weight of PS-*b*-PMMA at the similarly symmetric composition, the binary mixtures of PS-*b*-PMMAs were prepared by the freeze-drying method from polymer solution. For instance, a predetermined amount of mixture was dissolved in benzene (~10 wt % in solute) as a cosolvent and the quenched solution was evaporated under vacuum for 24 h, followed by sequential annealing at $T = 140-150$ °C for 24 h to thermally equilibrate the sample and to remove the solvent completely.

The order-to-disorder transition (ODT) temperatures for PS-*b*-PMMAs and their binary mixtures were measured during heating by Synchrotron SAXS experiments at 4C1 and 4C2 beamlines at the Pohang Light Source (PLS), Korea. The wavelength (λ) of the X-ray beam was 1.608 Å, and the energy resolution ($\Delta\lambda/\lambda$) was 1.5×10^{-2}. A 2D-CCD camera (Princeton Instruments Ins., SCX-TE/CCD-1242) was used to collect the scattered X-rays. Experimental conditions were set to be a typical beam size of 1 × 1 mm^2, sample-to-detector distance of 3 m, and sample thickness of 1.5 mm by compression-molding at 130−140 °C after thermal annealing. Moreover, the depolarized light scattering (DLS) was used to confirm the ODT temperatures using a polarized beam from a He−Ne laser at a wavelength of 632.8 nm, where the intensity detected at photodiode through A/D converter was recorded as a function of temperature. All the heating processes were controlled automatically by a PID controller at constant heating rate 1.0 °C/min from 120 to 250 °C under the nitrogen flow to avoid thermal degradation of the polymer samples.

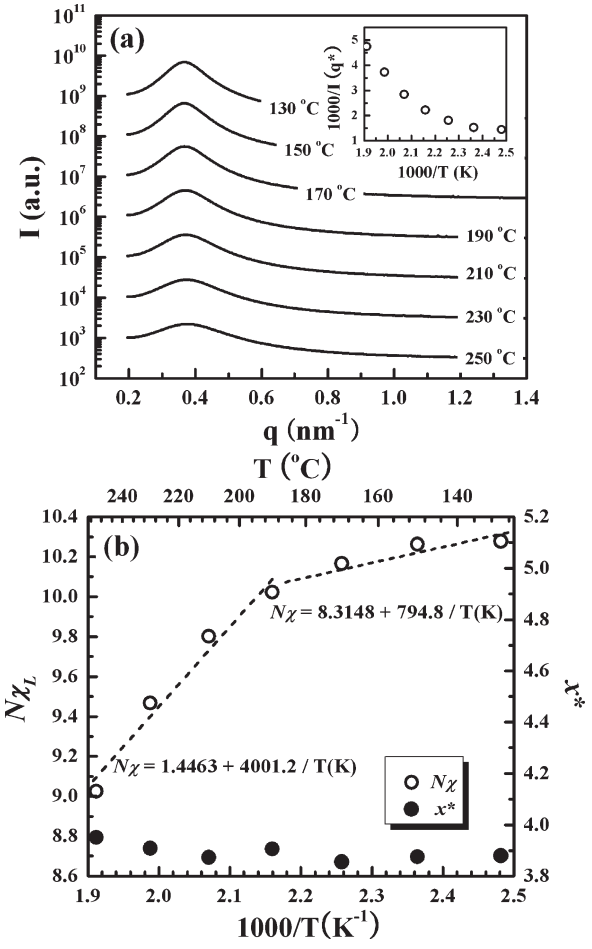

Figure 1. (a) SAXS intensity profiles for disordered PS-*b*-PMMA-20.0p as a function of scattering vector (q) at various temperatures ranging from 130 to 250 °C. The inset gives the inverse of the scattering intensity maximum ($1/I(q^*)$) plotted against inverse temperature ($1/K$); (b) Experimental $N\chi_L$ (○) as a function of the inverse of temperature, where $N\chi_L$ is extracted from the SAXS intensity profiles by comparing them with Leibler's scattering function. $N\chi_L$ is fitted to a linear equation as $N\chi_L = 1.4463 + 4001.2/T$, when $T \geq 190$ °C ($1/T \leq 0.00216$), and as $N\chi_L = 8.3418 + 794.8/T$, when $T \leq 190$ °C ($1/T \geq 0.00216$). The characteristic squared wavenumber x^* ($\equiv (q^*R_g)^2$; ●) is drawn together.

Results and Discussion

SAXS intensity profiles for PS-*b*-PMMA-20.0p of the lowest molecular weight, measured at various temperatures during heating from 130 to 250 °C, are shown in Figure 1a as a function of the scattering vector (q), where $q = (4\pi/\lambda)\sin\theta$, 2θ and λ are the scattering angle and wavelength, respectively. A broad and diffuse maximum over the entire temperature range indicates the characteristic correlation hole scattering arising from a disordered (or phase-mixed) state of the block copolymer melts. A detail in inset illustrates a nonlinear relationship with inverse temperature, although a gradual decrease of the maximum intensity with increasing temperature corresponds to an ODT-type phase behavior of block copolymers.

We attempt to elicit the empirical effective Flory parameter $\chi_L(T)$ by fitting the scattering intensity $I(q)$ to the Leibler's incompressible scattering function $S(q)$.[19] The $I(q)$ is given by $I(q) = k_n \times S(q)$, where k_n is the contrast factor. The $S(q)$ of a diblock copolymer melt is given as $S(q)^{-1} = 2N\chi_s - 2N\chi_L$, where $2N\chi_s$ is obtained from the Gaussian i,j-correlation functions S^0_{ij} as $\sum S^0_{ij}/\det(S^0_{ij})$. To get rid of the contrast factor, $I(q)$ is divided by its maximum, $I_{max}(q^*)$, at a characteristic wavenumber q^*. Then,

$I(q)/I_{max}$ becomes

$$I(q)/I_{max} = \frac{2N\chi_s(q^*) - 2N\chi_L}{2N\chi_s(q) - 2N\chi_L} \quad (1)$$

When a simple nonlinear regression routine is used, $N\chi_L$ is extracted from eq 1 and then plotted against the inverse of temperature in Figure 1b. $N\chi_L$ is often fitted to a linear equation as $N\chi_L = c + d/T$ with entropic parameter c and enthalpic parameter d. However, it is seen that $N\chi_L$ cannot be fitted to a single line over the whole temperature range. To simplify its temperature dependence, the $N\chi_L$ plot is divided into two regions. In the region of higher four temperatures (190−250 °C), it is obtained that

$$N\chi_L = 1.4463 + 4001.2/T \quad (2)$$

It is seen in eq 2 that the enthalpic contribution in $N\chi_L$ is stronger than the entropic contribution. This observation is in a sharp contrast to those previously reported. In a later section, we will show that χ in eq 2 is consistent with the determined ODT for the copolymers of higher molecular weights and also with our employed theory. If the data in the region of lower four temperatures (130−190 °C) are used, a whole different set of c and d is obtained as

$$N\chi_L = 8.3418 + 794.8/T \quad (3)$$

The above equation[48] is quite comparable to those reported by Hashimoto and co-workers[44] and by other groups with a strong entropic contribution and weak enthalpic contribution.[42,43] Would it be the fluctuation effects (random thermal noise)[44,49] that weaken the mean-field $N\chi_L$ for a disordered sample below a certain temperature (T_{MF})? We plotted the squared characteristic wavenumber x^* ($\equiv (q^*R_g)^2$ with gyration radius R_g) against temperature in Figure 1b. It is seen that there is no distinct variation in x^*, which implies that the whole experiment on PS-*b*-PMMA-20.0p has been done at $T > T_{MF}$.[50] For copolymer of $M = \sim$26000, Hashimoto and co-workers reported that $T_{MF} = \sim$180 °C. At least, T_{MF} here should be far lower than ∼180 °C, because the molecular weight of our sample is lower than that of the copolymer used in their experiments. It is the peculiar temperature dependence of $N\chi_L$ that causes such discrepancy in $N\chi_L$ and also the strong entropic contribution. In other words, linear fitting results for $N\chi_L$ depend on in what temperature range data are chosen.

Figure 2 shows SAXS intensity profiles and scattering parameters for PS-*b*-PMMA-29.2, measured at a heating rate of 1.0 °C/min from 160 to 242 °C. At lower temperatures ($T <$ 200 °C), a sharp scattering peak at $q^* = \sim$0.296 nm^{-1} and the second-order peak located at $2q^*$ relative to the primary peak are indicative of the microphase separation by the unfavorable interactions between two blocks, characteristic of the lamellar microdomain morphology. As temperature increases ($T >$ 200 °C), the primary peak remarkably weakens and broadens, holding further up a diffuse maximum at higher temperatures, which are consistent with the correlation hole scattering of a disordered block copolymer melt. This behavior is typical for block copolymers undergoing a transition from order to disorder. An ODT temperature of T = 200 °C for PS-*b*-PMMA-29.2 can be distinctly determined from the discontinuous changes in the scattering parameters, such as the inverse of the maximum intensity ($1/I(q^*)$), full-width at half-maximum (FWHM), and d-spacing (d) by $d = 2\pi/q^*$ as a function of inverse temperature ($1/K$), which are plotted in Figure 2b. As soon as temperature goes over 200 °C, $1/I(q^*)$ and FWHM increase and d-spacing decreases gradually, leading to the fact that the interaction

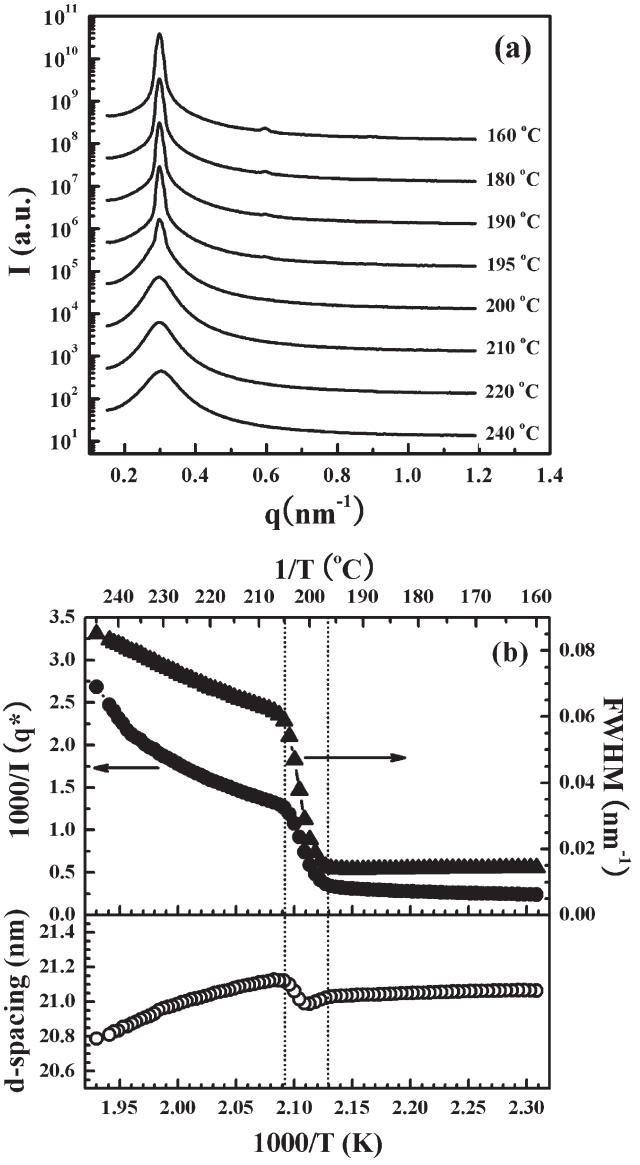

Figure 2. (a) SAXS intensity profiles for PS-*b*-PMMA-29.2 various temperatures during heating at a heating rate of 1.0 °C/min from 160 to 242 °C. To avoid overlapping, the intensity profiles were vertically shifted by a factor of 10. (b) The scattering parameters obtained from SAXS profiles. The inverse of a maximum intensity ($1/I(q^*)$), full-width at half-maximum (fwhm), and d-spacing calculated by $d = 2\pi/q^*$ are plotted as a function of inverse temperature ($1/K$). The dashed lines indicate transition range of PS-*b*-PMMA-29.2.

parameter (χ) between the two blocks of PS-*b*-PMMA decreases and the thermal fluctuation increases with increasing temperature.

In support of ODT evaluation for PS-*b*-PMMAs, we measured the depolarized light scattering (DLS) because it allows us to probe the transitions effectively due to the change between birefringent lamellar microdomains and isotropic disordered state of block copolymers. Figure 3 depicts such intensities as a function of temperature depending upon the molecular weight of PS-*b*-PMMAs. For PS-*b*-PMMA-29.2, the intensity at lower temperatures ($T <$ 200 °C) was observed due to the optical anisotropy of the lamellar microdomains, which is followed by a sharp decrease in the intensity at ODT of $T \sim$ 200 °C to zero, remaining disordered with further increasing temperature up to 250 °C. It is notable that this ODT evaluation is in accordance with that (200 °C) measured by SAXS when the transitions are taken at the starting point in the DLS intensity. The difference of

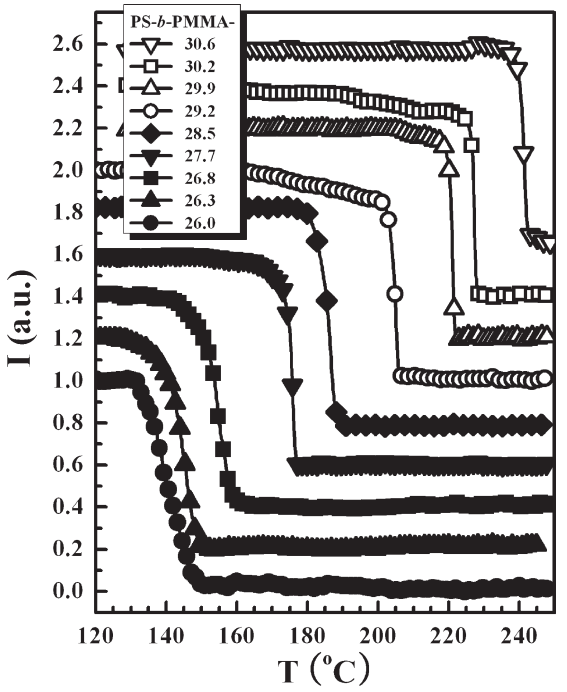

Figure 3. Depolarized light scattering (DLS) intensity as a function of temperature for the various PS-*b*-PMMAs depending upon the molecular weight. All intensities were measured during heating at a heating rate of 1.0 °C/min from 120 to 250 °C. For clarity, intensity profiles are vertically shifted.

the two transition temperatures between these two methods may arise from ether the broad transitions or the different measurement procedures within the experimental error range of ± 2 °C. A broader transitional range for PS-*b*-PMMA-26.0 can be attributed to the restricted chain mobility of block copolymer due to the approach to the glass transition temperatures of the PS (100 °C) and the PMMA block (115 °C). It should also be mentioned that with respect to PS-*b*-PMMA-28.5p, only ~30% decrease of molecular weight to 20000 g/mol leads to a disordered state of PS-*b*-PMMA, while ~25% increase of molecular weight to 35600 g/mol yields a fully ordered state up to 250 °C. However, the lowest and highest molecular weights for accessible ODT for PS-*b*-PMMA, as shown in Figure 3, were substantially 26000 and 30600 g/mol, which correspond to a 9% decrease and a 7% increase of molecular weight based on 28500 g/mol, respectively. The small changes in molecular weight of the copolymers are not prone to influencing the polydispersity.[51]

Figure 4 shows the molecular weight dependence of the ODT temperatures for PS-*b*-PMMAs with molecular weights from M = 26000 to 30600 g/mol. As the molecular weight of the mixed samples increases, the ODT temperatures, measured by DLS and SAXS, gradually increase with a rate of ΔT_{ODT} = ~100 °C over ΔM = 4600 g/mol. It should be noted here that the volume fraction of PS in the PS-*b*-PMMAs are kept constant with a nearly symmetric composition, confirming a lamellar morphology.

Let us discuss the ordering transition behavior using the compressible RPA model recently developed by one of us to elicit the effective Flory interaction parameter χ_F, which is of our central interest. We consider A-*b*-B diblock copolymers with N_i monomers of i-type with a total number of segments, $N (= \sum N_i)$. Block copolymer chains are assumed to be perturbed hard sphere chains of uniform diameter σ in a continuum. The nonbonded perturbed i,j-interactions are characterized by ε_{ij}. A hard-core volume fraction of i-monomers of the block copolymer chain is defined by $\phi_i \equiv N_i/N$. The fraction of free volume in the system is

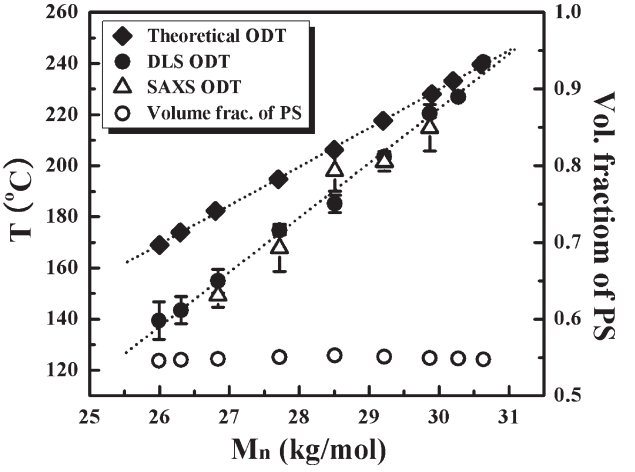

Figure 4. Comparison of measured ODT's using SAXS (△) and DLS (●) along with those given by theory (♦) for PS-*b*-PMMAs of various molecular weights. It is also shown that the volume fraction (○) of PS in the PS-*b*-PMMAs are consistent with a nearly symmetric composition, confirming a lamellar morphology.

denoted by η_f and the total packing density, that is, the fraction of volume occupied by all the monomers, is $\eta = 1 - \eta_f$.

We use a mean-field Landau analysis to study weakly phase segregating block copolymer systems. δF, the difference in free energies between ordered and disordered states, can be expanded in a power series with the thermally averaged order parameters, $\bar{\psi}_1(\vec{r})$ ($\equiv 1/2\eta(\langle\eta_A(\vec{r}) - \eta_A\rangle - \langle\eta_B(\vec{r}) - \eta_B\rangle)$) for ordered profile and $\bar{\psi}_2(\vec{r})$($\equiv -\langle\eta_f(\vec{r}) - \eta_f\rangle$) for free volume, where $\eta_i(\vec{r})$ and $\eta_f(\vec{r})$ are, respectively, the local packing density of i-monomers and the local free volume fraction. The δF is then rewritten as a power series in the Fourier transform of $\bar{\psi}_1(\vec{q})$ and $\bar{\psi}_2(\vec{q})$, with the mth-order vertex functions $\bar{\Gamma}^{(m)}_{i...j}$ as its coefficients. After $\bar{\psi}_i(\vec{q})$ is written in polar form, a minimization procedure leads to a Landau free energy expansion only in more strongly fluctuating $\bar{\psi}_1(\vec{q})$ with effective vertex terms as its coefficients at a characteristic wavenumber q^*. The effective quadratic coefficient, denoted as Γ'_2, is given by $\Gamma'_2 = \eta[2\chi_s - 2\chi_F]$, where an effective Flory-type interaction parameter χ_F is subdivided into $\chi_F = \chi_{app} + \chi_{comp}$. The former is the density-dependent exchange energy term as $\chi_{app} \sim [\varepsilon_{AA} + \varepsilon_{BB} - 2\varepsilon_{AB}] \times \mu(\eta)/kT$, where $\mu(\eta)$ describes the density dependence of the attractive nonbonded interactions[52] and k is Boltzmann's constant. The latter is given as $\chi_{comp} \approx (\pi\sigma^3/6\eta) \times P^2_\phi/2kTB_T$ for the symmetric copolymer in the long chain limit, where P_ϕ ($= \partial P/\partial\phi)_{T,\nu}$) and B_T are, respectively, the disparity in equation-of-state properties between constituents and the isothermal bulk modulus.[40] More detailed description of the compressible Landau free energy is given in the Supporting Information (SI).

The model requires three homopolymer parameters: the self-interaction parameter ε_{ij}, σ_i, and N_i. In our previous work on the series of PS-*b*-poly(*n*-alkyl methacrylates), the required homopolymer parameters were tabulated.[43] From ref 43, each set of homopolymer parameters for either PS (A) or PMMA (B) are given as follows: $\sigma_A = \sigma_B = 4.04$ Å; $h_z\varepsilon_{AA}/k = 4107.0$ K, $h_z\varepsilon_{BB}/k = 4388.3$ K; $N_A\pi\sigma^3_A/6M_A = 0.41857$ cm^3/g, $N_B\pi\sigma^3_B/6M_B = 0.37757$ cm^3/g, where h_z (≈10) denotes the number of nonbonded nearest neighbors around a chosen monomer. There is then ε_{AB} left for cross interaction between different polymers, which is the *sole adjustable parameter* and determined by fitting phase behavior of a given block copolymer system.

The present model takes a united atom-type description of real polymer chains, so that no detailed pendant groups are taken into consideration. An average force field is assumed to act as interactions between the spherical i- and j-monomers.

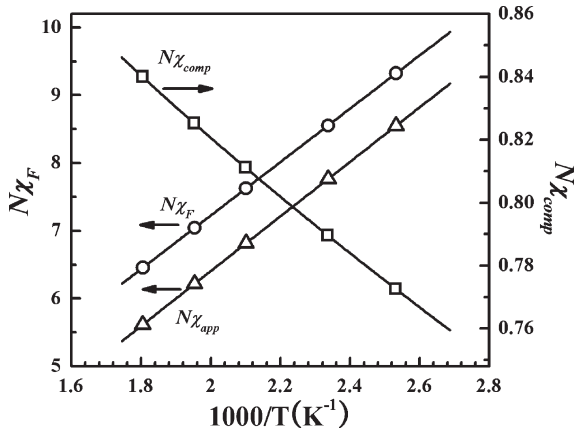

Figure 5. $N\chi_F$ plotted against inverse temperature for the fully disordered PS-*b*-PMMA (PS-*b*-PMMA-20.0p) at ambient pressure. Its two components, $N\chi_{app}$ and $N\chi_{comp}$, are plotted together.

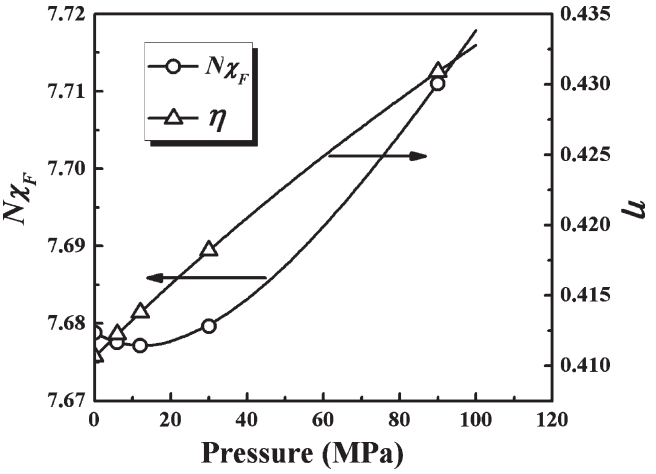

Figure 6. $N\chi_F$ (○) plotted as a function of pressure up to 100 MPa for the fully disordered PS-*b*-PMMA (PS-*b*-PMMA-20.0p) at 200 °C, revealing baroplasticity at the early stage and then barotropicity in the remaining. To understand its behavior, the overall density η (△) is drawn together.

We attempt to obtain the cross-interaction parameter ε_{AB} in the vicinity of the conventional Berthelot's rule ($\varepsilon_{AB} = (\varepsilon_{AA}\varepsilon_{BB})^{1/2}$). Not to invoke any complicated numerical regression scheme, we simply choose the copolymer with the highest ODT from Figure 4, which is the case of PS-*b*-PMMA-30.6 with $M = 30600$. Using the free energy given in the SI, ε_{ij} is then adjusted to ($\varepsilon_{AB} = 0.99821\text{-}(\varepsilon_{AA}\varepsilon_{BB})^{1/2}$) from fitting the ODT. Dipole of phenyl ring and induced dipole of the polar ester group of lower alkyl methacrylates can form directional interactions, though weak, as was discussed in our previous publication.[43] However, PS-*b*-PMMA is certainly too rigid to associate or dissociate directional pairs. It is then quite natural for us to take ε_{AB} around the Berthelot's rule, which is frequently used for the determination of cross interactions in nonpolar polymer mixtures. In Figure 4, we compare ODTs from the experiments and from the present theory as a function of the copolymer molecular weight. Because the ODT from the scattering data for the copolymer of $M = 30600$ was used to obtain ε_{ij} for theory, the lines of ODTs from two different approaches coincide at that molecular weight. With the change in the copolymer molecular weight by 4600 g/mol, the ODT from the experiments shifts by ~100 °C. Theory also reveals such a moderate change in ODT, even though its rate is slower than the experimental observation. However, it should be noted that only a single point is used to elicit the cross interaction parameter. To fit the data perfectly, it is necessary to slightly increase ε_{AB} or, equivalently, reduce the unfavorable interaction $\Delta\varepsilon$ ($\equiv \varepsilon_{AA} + \varepsilon_{BB} - 2\varepsilon_{AB}$), as the copolymer molecular weight is lowered.[53]

With the chosen ε_{AB}, $\Delta\varepsilon/k$ becomes 1.986 K. χ_{app} is of course a decreasing function of temperature. Its temperature dependence is modified by $\mu(\eta)$, which is also a decreasing function of temperature due to the density η. Meanwhile, $|\varepsilon_{AA} - \varepsilon_{BB}|$ for PS-*b*-PMMA is merely less than 7% of ε_{AA}. As the self-interaction strength mostly determines compressibility of block component, P_ϕ is thus small and so is χ_{comp}. Owing to the decrease of B_T with temperature, however, χ_{comp} becomes a gradually increasing function of temperature. Such temperature dependence of the two contributions to χ_F at ambient pressure for the copolymer of $M = 20000$ with $\phi_{PS} = 0.55$ is depicted in Figure 5. As can be seen, χ_{comp} is only 8−15% of χ_{app} in the given temperature range, so that χ_F also shows temperature dependence similar to χ_{app}.

For the quick comparison with the present experiment, we fit χ_F in Figure 5 to a typical linear equation as

$$N\chi_F = -0.6577 + 3942.1/T \quad (4)$$

It can be seen that eq 4 is quite consistent with the experimental $N\chi_L$ in eq 2, obtained using the data points at higher temperatures. χ_F is again described mostly by the enthalpic parameter *d*. If χ_F (or χ_L) were dominated by entropic contribution, ODT might be drastically changed upon a slight change in copolymer molecular weight. The moderate rate of ODT change for PS-*b*-PMMA in Figure 4 then justifies the dominance of enthalpic contribution as in eq 2 or 4. Now, it raises a question why the copolymer reveals reduction in $N\chi_L$ when temperature is lowered but still in the mean-field regime. This observation seems also correlated with the fact that $\Delta\varepsilon$ from theory becomes less unfavorable for the copolymer with lower ODT. There may be some role of the polar ester group of PMMA either by weak interaction effects between it and the phenyl ring of PS, which we ignore here, or by potential moisture uptake, which can also alter energetics. There is a definite need for further investigation by using scattering and also spectroscopy for so common but still peculiar PS-*b*-PMMA copolymer system.

In addition, let us consider the effect of pressure on χ_F, where there is also discrepancy in the reported behaviors.[45−47] Figure 6 shows χ_F at 200 °C for the same copolymer used in the previous figure, plotted against pressure. Unlike the temperature dependence of χ_F, the response of the copolymer to pressure is somewhat complicated. As the copolymer is pressurized, the density increases and so does the bulk modulus B_T contrary to their temperature responses. χ_{app} increases accordingly due to the increased pair contact density. As $\Delta\varepsilon$ or χ_{app} is rather weak, the diminished χ_{comp} due to the strengthened B_T causes χ_F to decrease (baroplastic) with pressure in the early stage ($P < \sim 140$ bar). However, further increase in pressure makes χ_{app} effect take over χ_{comp}. Therefore, the copolymer becomes barotropic with the increased χ_F in its overall trend upon $\Delta P = 1000$ bar. The scattering measurements on the disordered PS-*b*-PMMA by Ruzette et al. show that the scattering intensity monotonically increases with pressure, even though no measurements have been made at pressures between 1 and 160 bar. Theory is then consistent with the experiment except the early stage of pressurization. Regarding the baroplastic response of the copolymer at lower pressures, though not supported by experimental observation, it is recalled that Freed predicted the copolymer to be baroplastic. We found that a slight reduction in $\Delta\varepsilon$ can enlarge pressure range for the baroplastic region. These theoretical results imply that the copolymer, though barotropic in its overall pressure dependence, is in the vicinity of a borderline separating baroplasticity and barotropicity.

Concluding Remarks

It has been shown for PS-*b*-PMMA diblock copolymer by using SAXS and DLS experiments and also by employing a mean-field theory that the effective Flory χ unveils its peculiar behavior depending on thermodynamic variables. The SAXS intensity profiles for a fully disordered PS-*b*-PMMA copolymer (M = 20000) were used to fit Leibler's scattering function to obtain empirical χ_L as a function of temperature. The intensity data at higher temperatures (190 − 250 °C) yielded χ_L mostly described by enthalpic contribution, unlike χ previously reported in the literature, where its entropic contribution was substantial. In the lower temperature range (130−190 °C), χ_L began to have stronger entropic contribution similar to the literature χ. We directly measured ODTs for the copolymers of the controlled molecular weights (M = 26000−30600) using SAXS and DLS techniques. The resultant transition temperatures were analyzed with the compressible random-phase approximation (RPA) theory. When our theory was used, effective χ_F was determined by a slight adjustment of simple Berthelot's rule for the cross interaction ε_{AB} to fit ODT. It was found that χ_F from theory is also mostly described by its enthalpic contribution, which yields a moderate change in ODT (ΔT_{ODT} = ∼70 °C theoretically, while ΔT_{ODT} = ∼100 °C experimentally) upon molecular weight change (ΔM = 4600). In addition, it was shown from theoretical χ_F that the pressure response of the copolymer is slightly baroplastic initially, then turns to be barotropic, which implies that the increase of unfavorable energetics due to the increased contact density soon prevails as the action of the copolymer against pressure. Therefore, the copolymer becomes barotropic with the increased χ_F in its overall trend upon ΔP = 1000 bar, which is consistent with the earlier observation by Ruzette et al.

Acknowledgment. This work has been supported by Korea Research Foundation [20090064714]. J.C. also acknowledges the support from the GRRC program of Gyeonggi province [GRRCdankook2009-B04]. D.Y.R acknowledges the financial support from APCPI ERC program (R11-2007-050-02001) funded by the Ministry of Education, Science & Technology (MEST).

Supporting Information Available: Detailed description of the chosen compressible RPA model. This material is available free of charge via the Internet at http://pubs.acs.org.

References and Notes

(1) Jeong, B.; Bae, Y. H.; Lee, D. S.; Kim, S. W. *Nature* **1997**, *388*, 860.
(2) Park, M.; Harrison, C.; Chaikin, P. M.; Register, R. A.; Adamson, D. H. *Science* **1997**, *276*, 1401.
(3) Foster, S. M. A. *Adv. Mater.* **1998**, *10*, 195.
(4) Discher, B. M.; Won, Y.-Y.; Ege, D. S.; Lee, J. C.-M.; Bates, F. S.; Discher, D. E.; Hammer, D. A. *Science* **1999**, *284*, 1143.
(5) Zehner, R. W.; Sita, L. R. *Langmuir* **1999**, *15*, 6139.
(6) Li, R. R.; Dapkus, P. D.; Thompson, M. E.; Jeong, W. G.; Harrison, C.; Chaikin, P. M.; Register, R. A.; Adamson, D. H. *Appl. Phys. Lett.* **2000**, *76*, 1689.
(7) Thurn-Albrecht, T.; Schotter, J.; Kastle, G. A.; Emley, N.; Shibauchi, T.; Krusin-Elbaum, L.; Guarini, K.; Black, C. T.; Tuominen, M. T.; Russell, T. P. *Science* **2000**, *290*, 2126.
(8) Black, C. T.; Guarini, K. W.; Milkove, K. R.; Baker, S. M.; Russell, T. P.; Tuominen, M. T. *Appl. Phys. Lett.* **2001**, *79*, 409.
(9) Cheng, J. Y.; Ross, C. A.; Chan, V. Z.-H.; Thomas, E. L.; Lammertink, R. G. H.; Vancso, G. J. *Adv. Mater.* **2001**, *13*, 1174.
(10) Liu, K.; Baker, S. M.; Tuominen, M.; Russell, T. P.; Schuller, I. K. *Phys. Rev. B* **2001**, *63*, 060403.
(11) Lopes, W. A.; Jaeger, H. M. *Nature* **2001**, *414*, 735.
(12) Shin, K.; Leach, K. A.; Goldbach, J. T.; Kim, D. H.; Jho, J. Y.; Tuominen, M.; Hawker, C. J.; Russell, T. P. *Nano Lett.* **2002**, *2*, 933.
(13) Yang, S. Y.; Park, J.; Yoon, J.; Ree, M.; Jang, S. K.; Kim, J. K. *Adv. Funct. Mater.* **2008**, *18*, 1371.
(14) Hadjichristidis, N.; Pispas, S.; Floudas, G. A. *Block Copolymers: Synthetic Strategies, Physical Properties, and Applications*; John Wiley & Sons, Inc.: Hoboken, NJ, 2003.
(15) Hamley, I. W., Ed. *Developments in Block Copolymer Science and Technology*; John Wiley & Sons Ltd.: Chichester, England, 2004.
(16) Bates, F. S.; Fredrickson, G. H. *Annu. Rev. Phys. Chem.* **1990**, *41*, 525.
(17) Hashimoto, T. In *Thermoplastic Elastomers*; Holden, G., Legge, N. R., Quirk, R. P., Schroeder, H. E., Eds.; Hanser: New York, 1996.
(18) Hamley, I. W. *The Physics of Block Copolymers*; Oxford University Press, Inc.: New York, 1998.
(19) Leibler, L. *Macromolecules* **1980**, *13*, 1602.
(20) Ohta, T.; Kawasaki, K. *Macromolecules* **1986**, *19*, 2621.
(21) Fredrickson, G. H.; Helfand, E. *J. Chem. Phys.* **1987**, *87*, 697.
(22) Mayes, A. M.; Olvera de la Cruz, M. *J. Chem. Phys.* **1991**, *95* (6), 4670.
(23) Barrat, J.-L.; Fredrickson, G. H. *J. Chem. Phys.* **1991**, *95* (2), 1281.
(24) Helfand, E. *J. Chem. Phys.* **1975**, *62*, 999.
(25) Hong, K. M.; Noolandi, J. *Macromolecules* **1981**, *14*, 727.
(26) Vavasour, J. D.; Whitmore, M. D. *Macromolecules* **1992**, *25*, 5477.
(27) Matsen, M. W.; Schick, M. *Phys. Rev. Lett.* **1994**, *72*, 2660.
(28) McMullen, W. E.; Freed, K. F. *Macromolecules* **1990**, *23*, 255.
(29) Tang, H.; Freed, K. F. *J. Chem. Phys.* **1991**, *94*, 1572.
(30) Dudowicz, J.; Freed, K. F. *Macromolecules* **1993**, *26*, 213.
(31) Freed, K. F.; Dudowicz, J. *J. Chem. Phys.* **1992**, *97*, 2105.
(32) Dudowicz, J.; Freed, K. F. *Macromolecules* **1995**, *28*, 6625.
(33) Yeung, C.; Desai, R. C.; Shi, A. C.; Noolandi, J. *Phys. Rev. Lett.* **1994**, *72*, 1834.
(34) Bidkar, U. R.; Sanchez, I. C. *Macromolecules* **1995**, *28*, 3963.
(35) Hino, T.; Prausnitz, J. M. *Macromolecules* **1998**, *31*, 2636.
(36) Cho, J. *Macromolecules* **2001**, *34*, 1001.
(37) Cho, J. *J. Chem. Phys.* **2003**, *119*, 5711.
(38) Cho, J. *Macromolecules* **2004**, *37*, 10101.
(39) Cho, J.; Wang, Z.-G. *Macromolecules* **2006**, *39*, 4576.
(40) Cho, J. *Polymer* **2007**, *48*, 429.
(41) Ryu, D. Y.; Shin, K.; Drockenmuller, E.; Hawker, C. J.; Russell, T. P. *Science* **2005**, *308*, 236.
(42) Russell, T. P.; Hjelm, R. P.; Seegar, P. A. *Macromolecules* **1990**, *23*, 890.
(43) Ryu, D. Y.; Shin, C.; Cho, J.; Lee, D. H.; Kim, J. K.; Lavery, K. A.; Russell, T. P. *Macromolecules* **2007**, *40*, 7644.
(44) Zhao, Y.; Sinaviah, E.; Hashimoto, T. *Macromolecules* **2008**, *41*, 9948.
(45) Freed, K. F.; Dudowicz, J. *Macromolecules* **1996**, *29*, 625.
(46) Freed, K. F.; Dudowicz, J.; Foreman, K. W. *J. Chem. Phys.* **1998**, *108*, 7881.
(47) Ruzette, A.-V.; Mayes, A. M.; Pollard, M.; Russell, T. P.; Hammouda, B. *Macromolecules* **2003**, *36*, 3351.
(48) As the average number of segments for PS-*b*-PMMA of M = 20000 at ϕ_{PS} = 0.55 is N = 196.4, χ_L is given from eq 3 as $\chi_L = 0.0425 + 4.046/T$.
(49) Sakamoto, N.; Hashimoto, T. *Macromolecules* **1995**, *28*, 6825.
(50) We were able to construct a master curve by vertically shifting all the inverse scattering intensities ($k_n/I(q)$ against $(q/q^*)^2$, where k_n is the contrast factor) in Figure 1 with the shifting factor of $2N\chi$, which ensures that the copolymer of M = 20000 is in the mean-field regime.
(51) In addition, the most disperse PS-*b*-PMMA mixture out of the pristine samples in Table 1, which is symmetrically composed of two extreme molecular weights of 20000 and 35600 g/mol to finally have 27800 g/mol in the number-average molecular weight and the polydispersity of 1.20, turns out to show an ODT at 213 °C. Compared with an ODT at 175 °C for PS-*b*-PMMA-27.7, whose molecular weight is very close to that given above, the ODT for this most disperse PS-*b*-PMMA mixture is overestimated by 38 °C, which can then be attributed to the polydispersity effect. However, such polydispersity effect on ODT for PS-*b*-PMMAs listed in Table 1 is not believed to be significant, because all the PS-*b*-PMMAs have the narrow distributions with polydispersity less than 1.09.
(52) The $\mu(\eta)$ in χ_{app} is defined as $\mu(\eta) = (\gamma/C)^4\eta^4 - (\gamma/C)^2\eta^2$ with $\gamma = 1/\sqrt{2}$ and $C = \pi/6$.
(53) $\Delta\varepsilon/k$ needs to be reduced by ∼8% to fit ODT for PS-*b*-PMMA-26.0 of M = 26000. If the concentration fluctuation effect ($N^{-1/3}$ dependence of $N\chi$ at ODT) is considered, $\Delta\varepsilon/k$ still needs to be reduced by ∼7% upon the given molecular weight decrease (ΔM = 4600).